Calcium influx selects the fast mode of endocytosis in the synaptic terminal of retinal bipolar cells

Guilherme Neves*†, Ana Gomis*‡, and Leon Lagnado§

Medical Research Council Laboratory of Molecular Biology, Hills Road, Cambridge CB2 2QH, United Kingdom

Edited by Charles F. Stevens, The Salk Institute for Biological Studies, La Jolla, CA, and approved October 16, 2001 (received for review June 20, 2001)

To investigate the regulation of endocytosis by Ca^{2+}, we have made capacitance measurements in the synaptic terminal of depolarizing bipolar cells from the retina of goldfish. After a brief depolarization, all of the excess membrane was retrieved rapidly ($\tau \approx 1$ s). But when the rise in free [Ca^{2+}] was reduced by the introduction of Ca^{2+} buffers [1,2-bis(2-aminophenoxy)ethane-*N,N,N′,N′*-tetraacetate (BAPTA) or EGTA], a large fraction of the membrane was retrieved by a second, slower mechanism ($\tau \geq 10$ s). The block of fast endocytosis by EGTA could be overcome by increasing the amplitude of the Ca^{2+} current, demonstrating that Ca^{2+} influx was the trigger for fast endocytosis. These manipulations of the Ca^{2+} signal altered the relative proportions of fast and slow endocytosis but did not modulate the rate constants of these processes. A brief stimulus that triggered fast endocytosis did not generate a significant rise in the spatially averaged [Ca^{2+}], indicating that Ca^{2+} regulated endocytosis through an action close to the active zone. The slow mode of retrieval occurred at the resting [Ca^{2+}]. These results demonstrate that Ca^{2+} influx couples fast endocytosis and exocytosis at this synapse.

At the synapse, rapid release of neurotransmitter occurs when Ca^{2+} enters the presynaptic terminal to trigger fusion of small vesicles (1, 2). The maintenance of normal synaptic transmission requires that these vesicles be retrieved (3), but it is unclear how endocytosis is modulated during synaptic activity (4–7). Here we provide a direct demonstration that Ca^{2+} influx triggering fast exocytosis also selects synaptic vesicles for fast retrieval.

Uncertainties about the properties of endocytosis at the synapse are in large part caused by the difficulties associated with measuring this process reliably (8–10). A real-time method is the capacitance technique, which allows changes in membrane surface area to be recorded with high temporal resolution. The capacitance technique cannot be applied to most synapses because of their small size, but we have used a neuron with a very large synaptic terminal, the depolarizing bipolar cell from the retina of goldfish. Using this preparation, it was demonstrated that retrieval of synaptic vesicles could occur within about 1 s (11). It was then shown that there were two kinetically distinct mechanisms of retrieval that could occur simultaneously: fast endocytosis with a rate constant of about 1 s^{-1} and slow endocytosis with a rate constant of about 0.1 s^{-1} (12). An increase in stimulus duration led to a decrease in the proportion of membrane retrieved by fast endocytosis and an increase in the proportion retrieved by slow endocytosis, without changing the rate constant of either process (12). A recent study has also observed fast and slow phases of endocytosis at the ribbon synapse of hair cells in the cochlea (13, 14).

Some studies have suggested that Ca^{2+} has no effect on endocytosis at the synapse (15, 16), whereas others indicate that Ca^{2+} is stimulatory (13, 17, 18), or inhibitory (19, 20). In the giant synaptic terminal of bipolar cells, capacitance measurements have been interpreted as indicating that Ca^{2+} inhibits endocytosis (21). Here we provide evidence that Ca^{2+} influx stimulates endocytosis at this synapse by triggering the fast mode of retrieval. This action of Ca^{2+} appears to be localized to the active zone. Vesicles that are not retrieved by the fast route are retrieved by slow endocytosis, which operates at resting levels of Ca^{2+}. The results provide a direct demonstration that Ca^{2+} influx couples fast exocytosis and endocytosis at the synapse.

Materials and Methods

Electrophysiology. Depolarizing bipolar cells from the goldfish retina were obtained by enzymatic dissociation (22). The standard Ringer's solution contained: 120 mM NaCl, 2.5 mM $CaCl_2$, 2.5 mM KCl, 1 mM $MgCl_2$, 10 mM glucose, and 10 mM Hepes (pH 7.3). The solution in the patch-pipette contained: 110 mM caesium gluconate, 4 mM $MgCl_2$, 3 mM Na_2ATP, 1 mM Na_2GTP, 10 mM tetraethylammonium chloride, and 20 mM Hepes (260 mosmol·liter^{-1}, pH 7.2). For conventional whole-cell recordings it was supplemented with EGTA (0.5–75 mM) or 1,2-bis(2-aminophenoxy)ethane-*N,N,N′,N′*-tetraacetate (BAPTA) (0.4 or 2 mM), as described in the text. When making perforated patch recordings, this solution was supplemented with 250 μg·ml^{-1} nystatin and 0.4 mM BAPTA. In the presence of 2 mM EGTA, the free [Ca^{2+}] in the pipette solution was ≈100 nM (measured with fura-2). In all experiments, the membrane potential was held at −70 mV, and stimuli were delivered by stepping the membrane potential to −10 mV. Brief stimuli lasted 20 ms, and long stimuli lasted 500 ms. All capacitance measurements were made in synaptic terminals detached from the axon during the dissociation procedure as described (12). Brief stimuli did not generate conductance changes. Long stimuli that caused a significant rise in bulk [Ca^{2+}] activated a Ca^{2+}-sensitive conductance, but calculations and experiments both indicate that this rise will not significantly corrupt measurements of the change in membrane capacitance (12).

In some experiments terminals were loaded with EGTA by incubation in 0.2 mM of the acetoxymethyl (AM) ester of EGTA (Molecular Probes) for 15–20 min (23). The final [EGTA] was estimated to be at least at 5 mM because it was sufficient to completely block bulk rises in free Ca^{2+} in response to long stimuli (24). Terminals were then washed in Ringer's solution lacking $CaCl_2$ for 10 min. Normal Ringer's solution containing $CaCl_2$ was replaced only after the terminal was voltage-clamped. Whole-cell dialysis often led to a gradual slowing of endocytosis, but this problem was minimized by confining measurements to a time window extending 2–5 min from the beginning of whole-cell recording.

Fitting of Traces. Visual inspection of capacitance records indicated that the fall in membrane surface area either occurred as

This paper was submitted directly (Track II) to the PNAS office.

Abbreviations: BAPTA, 1,2-bis(2-aminophenoxy)ethane-*N,N,N′,N′*-tetraacetate; AM, acetoxymethyl.

*G.N. and A.G. contributed equally to this work.

†Present address: Whitehead Institute for Biomedical Research, Nine Cambridge Center, Cambridge, MA 02142.

‡Present address: Instituto de Neurociencias, Universidad Miguel Hernández, Apartado 18, San Juan de Alicante 03550, Spain.

§To whom reprint requests should be addressed. E-mail: LL1@mrc-lmb.cam.ac.uk.

The publication costs of this article were defrayed in part by page charge payment. This article must therefore be hereby marked "*advertisement*" in accordance with 18 U.S.C. §1734 solely to indicate this fact.

www.pnas.org/cgi/doi/10.1073/pnas.261311698

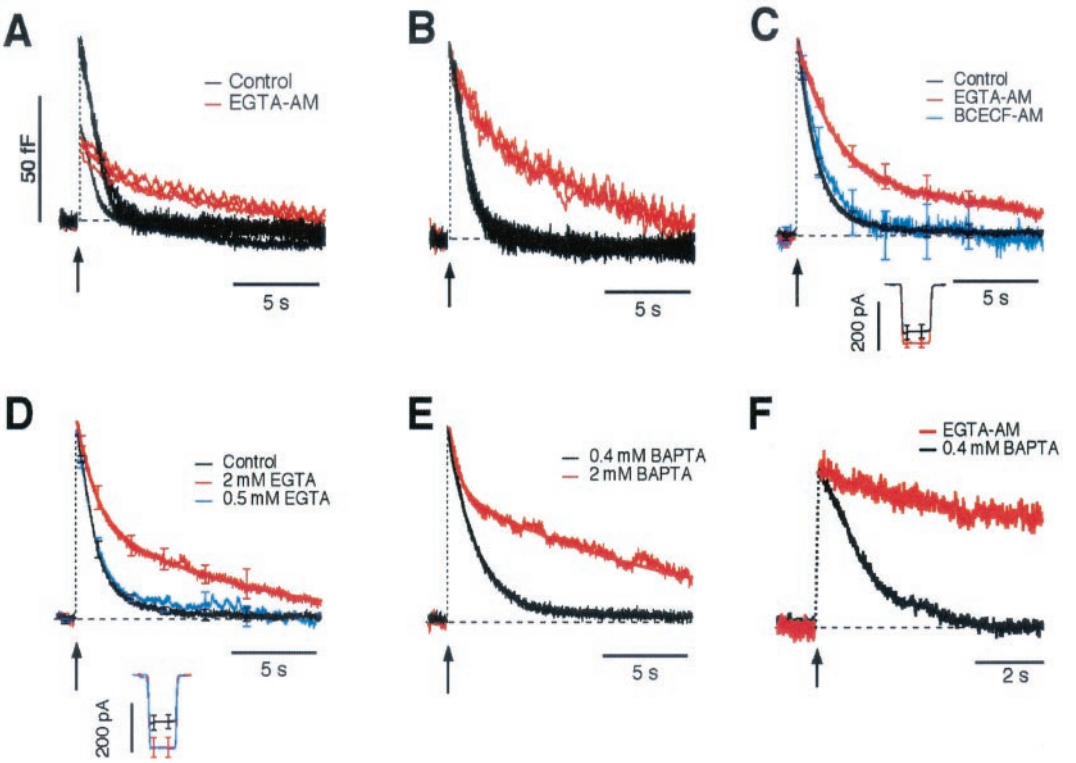

Fig. 1. Calcium buffers caused a proportion of synaptic vesicles to be retrieved by slow endocytosis. (*A*) Examples of capacitance responses elicited by a 20-ms depolarization to −10 mV (delivered at arrow), recorded by using the perforated patch technique. Compared are single responses in untreated terminals (black) and terminals incubated in EGTA-AM (red). (*B*) Responses from *A* scaled to the same maximum to allow direct comparison of the kinetics of endocytosis. (*C*) Averaged time courses of endocytosis from scaled responses in control terminals (black, $n = 10$), and terminals treated with EGTA-AM (red, $n = 16$) or the AM ester of the pH buffer BCECF [2′,7′-bis-carboxyethyl-5(6)carboxyfluorescein] (blue, $n = 6$). Bars show SEM at fixed time points. The bold black trace describing the time course of endocytosis in control terminals is a single exponential declining with $\tau = 1.2$ s. The bold red trace describing the time course of endocytosis in terminals treated with EGTA-AM is a double exponential with $A_{fast} = 64\%$, $\tau_{fast} = 2$ s, $A_{slow} = 36\%$, and $\tau_{slow} = 13.9$ s (see text). The peak amplitude of the capacitance responses was 57 ± 8 fF in controls and 50 ± 5 fF in terminals treated with EGTA-AM. (*Inset*) The averaged Ca^{2+} currents. (*D*) Kinetics of endocytosis after the same stimulus delivered in conventional whole-cell recordings with pipette solutions containing 0.5 mM EGTA (blue, $n = 6$) or 2 mM EGTA (red, $n = 10$). In 0.5 mM EGTA endocytosis occurred with $\tau = 1.3$ s and so was very similar to that observed in control experiments (the black trace is from *D*). The decline in membrane area in 2 mM EGTA could be described as a double exponential with $A_{fast} = 49\%$, $\tau_{fast} = 1.2$ s, and $\tau_{slow} = 11.2$ s (bold trace). (*E*) Comparison of averaged responses in 0.4 mM BAPTA (black, $n = 15$) and 2 mM BAPTA (red, $n = 9$). In 0.4 mM BAPTA endocytosis occurred with $\tau = 1.7$ s (bold trace) and so was very similar to that observed in control experiments (*D*). The decline in membrane area in 2 mM BAPTA could be described as a double exponential with $A_{fast} = 38\%$, $\tau_{fast} = 0.6$ s, and $\tau_{slow} = 13$ s. (*F*) The effects of excess EGTA could be reversed. The red trace is a single response measured in the perforated patch configuration after loading the terminal using EGTA-AM. The black trace is a record from the same terminal obtained 2 min after converting to the whole-cell configuration with 0.4 mM BAPTA in the pipette.

a single fast phase or as two phases, one fast and the other slow (Fig. 1). A useful way to compare measurements made under different conditions was to fit single or double exponential functions using the fitting procedure in IGOR PRO software (WaveMetrics, Lake Oswego, OR). Residual plots were examined to determine whether a double exponential function provided a substantially better description of the capacitance recovery than a single exponential. None of the parameters were constrained and initial guesses were automatically selected by the software.

Measurements of Free $[Ca^{2+}]$. Cells were loaded with fura-2 (Molecular Probes), either by introduction through the patch pipette (0.1 mM) or by incubation in 1 μM of the AM ester for 15 min. Ratiometric measurements of changes in $[Ca^{2+}]$ were made at wavelengths of 340 nm and 380 nm by using methods as described (12). In some experiments, the filter wheel was replaced by a monochromator-based illumination system (Cairn, Faversham, U.K.). The K_d of fura-2 was taken as 225 nM. To monitor the $[Ca^{2+}]$ in the terminal we also used Ca^{2+}-activated conductances in the surface membrane (24). This current is directly proportional to the average free $[Ca^{2+}]$, with a scaling factor of 9 pA/μM at a membrane potential of −70 mV (24). Bulk rises in free $[Ca^{2+}]$ can reach several micromolar in the bipolar cell terminal, causing the saturation of high-affinity dyes such as fura-2. Conversely, low-affinity dyes do not allow accurate measurement in the submicromoar range. Use of the Ca^{2+}-activated conductance allowed us to assay the bulk $[Ca^{2+}]$ over the whole of the normal range. Measurements are given as mean ± SEM.

Results

EGTA and BAPTA Blocked Fast Endocytosis. To investigate the role of Ca^{2+} during endocytosis we suppressed the rise in free $[Ca^{2+}]$ occurring during stimulation by introducing a Ca^{2+} chelator (EGTA or BAPTA) into the terminal. Fig. 1*A* shows examples of capacitance responses to a 20-ms depolarization to −10 mV, recorded by using the perforated patch technique. This stimulus was used for two reasons. First, it completely depletes a pool of rapidly releasable vesicles (12, 23, 25, 26), which are thought to be docked at the active zone (27). Second, independent measurements of exocytosis using the fluorescent dye FM1–43 demonstrate that there is negligible exocytosis after such a brief stimulus (12), allowing direct interpretation of capacitance

records as measures of endocytosis. The black traces are from terminals that only contain their endogenous Ca^{2+} buffers (termed controls), and the red traces are from terminals in which these buffers were augmented by applying EGTA-AM. To allow direct comparison of the rate constants of endocytosis, individual records were normalized to the same maximum (Fig. 1*B*). The averaged records after normalization are shown in Fig. 1*C*. In controls, all of the exocytosed membrane was retrieved with a time constant (τ) that averaged 1.2 ± 0.1 s (n = 10). But in terminals treated with EGTA-AM, the time course of retrieval was best described as the sum of two decaying exponentials. The bold red trace in Fig. 1*C* is of the form $A(t) = A_{fast}\cdot\exp(-t/\tau_{fast}) + A_{slow}\cdot\exp(-t/\tau_{slow})$, where $A(t)$ is the amount of membrane remaining to be retrieved at time t after the stimulus, and A_{fast} = 64%, τ_{fast} = 2 s, A_{slow} = 36%, and τ_{slow} = 13.9 s. The simplest interpretation of this description is that a fraction of membrane (A_{fast}) is endocytosed by a fast mechanism, whereas the remainder is retrieved slowly. The action of EGTA-AM could be attributed to the buffering of Ca^{2+} ions rather than a direct inhibitory effect of AMs, because endocytosis was not altered by treatment with 2′,7′-bis-carboxyethyl-5(6)carboxyfluorescein-AM (BCECF-AM), an AM ester that does not bind Ca^{2+} (Fig. 1*C*, blue trace).

The kinetics of endocytosis were also measured when known concentrations of Ca^{2+} buffers were introduced through the pipette used to make conventional whole-cell recordings. In terminals dialyzed with 0.5 mM EGTA (Fig. 1*D*, blue trace), the capacitance response to a brief stimulus recovered with τ = 1.1 ± 0.1 s (n = 6), which was not significantly different from that measured in controls (Fig. 1*D*, black trace). Increasing the EGTA concentration to 2 mM had an effect very similar to treatment with EGTA-AM; a proportion of membrane was retrieved slowly. The fitted red trace in Fig. 1*D* shows that 49% of the membrane was retrieved with τ_{fast} = 1.2 s, and the remainder with τ_{slow} = 11.2 s. BAPTA modulated endocytosis in a manner similar to EGTA. In terminals dialyzed with 0.4 mM BAPTA (Fig. 1*E*, black trace), the capacitance response to a brief stimulus recovered with τ = 1.7 ± 0.1 s (n = 15). But increasing the BAPTA concentration to 2 mM caused ~62% of the membrane to be retrieved with a time constant of ~13 s.

The effects of EGTA on the kinetics of endocytosis could not be attributed to a chronic reduction in resting [Ca^{2+}] because treatment with EGTA-AM did not cause significant changes in the resting [Ca^{2+}]. In a sample of six terminals loaded with the Ca^{2+} indicator fura-2 (using the AM ester), the resting [Ca^{2+}] was 59 ± 8 nM before treatment with EGTA-AM, and 71 ± 9 nM after. In a second sample of terminals dialyzed with 2 mM EGTA and 0.1 mM fura-2, the resting [Ca^{2+}] averaged 60 ± 15 nM (n = 6).

When recordings were made in the perforated patch configuration, a gradual suppression of fast endocytosis was observed by perfusion with EGTA-AM (seven terminals, results not shown). The effects of excess EGTA could then be reversed by removing the buffer through the patch pipette. Fig. 1*F* shows an example of such an experiment. The red trace is a response to a brief stimulus recorded in the perforated patch configuration after treatment with 500 μM EGTA-AM for 20 min. In this case, fast endocytosis was completely blocked. Converting to the whole-cell configuration with 0.4 mM BAPTA in the pipette caused recovery of fast retrieval within 2 min (Fig. 1*F*, black trace). Similar reversal of the effects of excess EGTA was observed in five terminals.

The results in Fig. 1 indicate that the Ca^{2+} signal normally generated by a brief stimulus caused all vesicles to be recycled rapidly, but counteracting the rise in free Ca^{2+} by the introduction of Ca^{2+} buffers caused a proportion of vesicles to be recycled by a second, slower mode of endocytosis. The fast and slow phases of endocytosis observed under different conditions of Ca^{2+} buffering had similar time constants to those previously observed in the presence of endogenous buffers (12). In that study it was found that the distribution of time constants allowed fast endocytosis to be defined as occurring with a time constant of 3 s or less, and slow endocytosis with a longer time constant (12). The results in Fig. 1 and Table 1 show that this 3-s cut-off also provides a simple and reliable definition for the two kinetically distinct mechanisms of membrane retrieval observed in the presence of alien Ca^{2+} buffers.

Table 1. Kinetics of endocytosis after a brief stimulus

	Control	0.5 mM EGTA	0.4 mM BAPTA	EGTA-AM	2 mM EGTA	2 mM BAPTA
A_{fast} (%)	100	100	100	64	49	38
τ_{fast} (s)	1.2	1.3	1.7	2	1.2	0.6
τ_{slow} (s)	—	—	—	14	11	13
n	10	6	15	16	10	9

The averaged time courses of the capacitance responses after a 20-ms depolarization were fit with the equation $A(t) = A_{fast}\cdot\exp(-t/\tau_{fast}) + A_{slow}\cdot\exp(-t/\tau_{slow})$. n is the number of terminals. Controls were recordings made by using the perforated patch technique without the addition of EGTA or BAPTA. In control terminals and terminals dialyzed with 0.5 mM EGTA or 0.4 mM BAPTA, the fall in capacitance could be described as a single exponential so the averaged record was fit with the equation $A(t) = A_{fast}\cdot\exp(-t/\tau_{fast})$.

Increased Ca^{2+} Influx Counteracted the Effects of Ca^{2+} Buffers. When the Ca^{2+} buffering capacity of terminals was increased, the kinetics of endocytosis became dependent on the amplitude of the Ca^{2+} current. Fig. 2*A* compares membrane retrieval after a brief stimulus in three different terminals, all loaded with 2 mM EGTA. When the Ca^{2+} current was weak, most of the membrane was retrieved slowly (Fig. 2*A*, black traces), but when the Ca^{2+} current was large, most of the membrane was retrieved rapidly (Fig. 2*A*, red traces). This trend is described in Fig. 2*B*, which plots the time to half-recovery ($t_{1/2}$) as a function of the amplitude of the Ca^{2+} current flowing during the 20-ms stimulus. The rate of endocytosis was not correlated with the amplitude of the Ca^{2+} current in control terminals (Fig. 2*B*, filled symbols). But in terminals loaded with excess EGTA (2–75 mM, Fig. 2*B*, open symbols), the largest Ca^{2+} currents were able to overcome the Ca^{2+} buffer and elicit endocytosis at rates similar to controls. Fitting these responses with double exponential functions, τ_{fast} varied between 0.5 and 2 s, and so could be easily differentiated from the slower phase of retrieval. Fig. 2*C* shows that larger Ca^{2+} currents accelerated the average rate of endocytosis by increasing the proportion of membrane retrieved by fast endocytosis.

The results in Figs. 1 and 2 indicate that Ca^{2+} influx modulates endocytosis at the synapse by a distinctive mechanism—the selection of vesicles for fast endocytosis.

Evidence That Fast Endocytosis Was Triggered by a Local Action of Ca^{2+}. Brief stimuli of the type used in Figs. 1 and 2 did not generate large changes in the free [Ca^{2+}] inside terminals. Fig. 3 shows two examples of measurements of the spatially averaged [Ca^{2+}] made with fura-2. In the terminal loaded with 0.4 mM EGTA and 0.1 mM fura-2, a 20-ms stimulus caused the [Ca^{2+}] to rise by ≈13 nM (Fig. 3 *A* and *C*). In the terminal loaded with 2 mM EGTA the rise in [Ca^{2+}] was <5 nM (Fig. 3 *B* and *C*). In similar measurements in eight terminals, the rise in [Ca^{2+}] generated by a 20-ms depolarization never exceeded 18 nM. It therefore seems unlikely that a global rise in [Ca^{2+}] is the signal selecting vesicles for fast endocytosis. Rather, these results suggest that fast endocytosis was triggered by an action of Ca^{2+} exerted close to Ca^{2+} channels in the plasma membrane.

EGTA binds Ca^{2+} ions relatively slowly ($k_{on} \sim 9 \times 10^6$ $M^{-1}\cdot s^{-1}$) and is expected to be ineffective as a Ca^{2+} buffer at

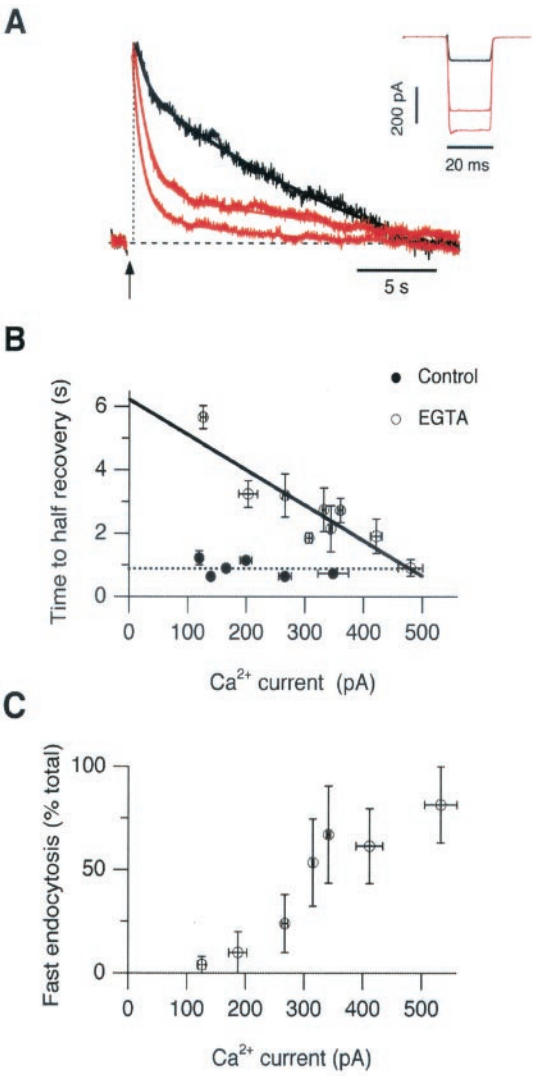

Fig. 2. Increasing Ca^{2+} influx counteracted the effects of EGTA and increased the amount of fast endocytosis. (*A*) Scaled capacitance responses elicited by brief stimuli in terminals loaded with 2 mM EGTA. The response in black (A_{fast} = 16%, τ_{fast} = 0.6 s, and τ_{slow} = 20 s) was elicited by a Ca^{2+} current of 140 pA (*Inset*). Larger Ca^{2+} currents (red traces) were associated with a larger proportion of fast endocytosis (85% and 63% in response to currents of 450 and 560 pA, respectively). (*B*) The time to half-recovery of the capacitance response ($t_{1/2}$) as a function of the Ca^{2+} current. In perforated patch recordings the kinetics of endocytosis were independent of the Ca^{2+} current (●, each n = 3). The average value of $t_{1/2}$ was 0.9 ± 0.1 s (n = 19). In terminals dialyzed with EGTA, $t_{1/2}$ was shorter for larger Ca^{2+} currents (○, each point n = 5). The line fitted to these measurements extrapolates to a $t_{1/2}$ of 6.2 s for the weakest Ca^{2+} currents. Results from terminals dialyzed with between 2 and 75 mM EGTA have been collected together because the kinetics of endocytosis were similar at all of these concentrations (see Fig. 4). Terminals treated with EGTA-AM displayed behavior similar to that seen in terminals loaded with 2 mM EGTA. (*C*) The percentage of membrane retrieved by fast endocytosis increased with larger Ca^{2+} currents. Single or double exponential functions were fitted to the recovery phase of the capacitance responses obtained in a total of 25 terminals loaded with 2–75 mM EGTA. In 11 terminals recovery was best described by a double exponential function, where τ_{fast} averaged 1.2 ± 0.2 s. In 14 terminals the whole recovery phase was adequately described with a single exponential function. In nine of these τ was longer than 3 s, and so recovery was considered all slow. In the remaining five, $\tau < 2$ s, recovery was considered all fast.

distances <20 nm from Ca^{2+} channels (28). As a result, EGTA has a limited ability to antagonize fast exocytosis at the synapse. In the synaptic terminal of bipolar cells, 2 mM EGTA blocks fast

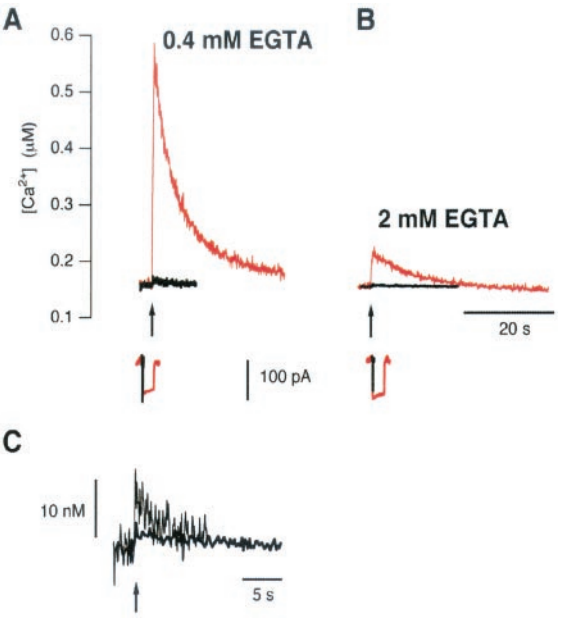

Fig. 3. Measurements of free $[Ca^{2+}]$ in the synaptic terminal. (*A*) Responses to depolarizations lasting 20 ms (bold black traces) and 500 ms (thin red traces) in a terminal dialyzed with 0.4 mM EGTA and 0.1 mM fura-2. (*B*) Responses from a terminal dialyzed with 2 mM EGTA and 0.1 mM fura-2. The corresponding Ca^{2+} currents are shown below. (*C*) Responses to 20-ms stimuli from *A* and *B* on expanded scales.

release of ~50% of vesicles in the rapidly releasable pool, whereas ≈20% of these vesicles are refractory to the effects of 40–75 mM EGTA (24). The block of fast endocytosis by EGTA was also limited by factors other than the concentration of the buffer. Fig. 4*C* plots the percentage of membrane retrieved by fast endocytosis as a function of the [EGTA] in the patch pipette. To assess the efficiency with which these varying concentrations of EGTA blocked fast endocytosis we limited our analysis to a sample of 35 terminals in which the amplitudes of the Ca^{2+} currents were similar (ranging from 210 to 310 pA). EGTA (2 mM) blocked fast retrieval of ~50% of the vesicles released by a brief stimulus, but 40 or 75 mM EGTA was not significantly more effective. These results suggests that the triggering of fast endocytosis was in large part a local action of Ca^{2+} that was not effectively blocked by a slow Ca^{2+} buffer. Note that the results in Fig. 4*C* could not be explained by assuming that a population of vesicles underwent fast endocytosis independent of Ca^{2+}, because fast retrieval could be completely blocked by reducing Ca^{2+} influx (Fig. 2*C*). The ability of EGTA to interfere with Ca^{2+}-triggered events at the active zone is not unexpected, given that vesicles at the active zone are docked over distances of a few hundred nanometers and EGTA is expected to be an effective buffer at distances 200 nm or more from Ca^{2+} channels (28).

BAPTA ($k_{on} \sim 6 \times 10^8\ M^{-1}\cdot s^{-1}$) is a faster Ca^{2+} chelator than EGTA and is therefore more effective at antagonizing the Ca^{2+} signal close to Ca^{2+} channels. At a concentration of 2 mM, BAPTA suppressed fast endocytosis somewhat more effectively than EGTA (Table 1), but we were not able to systematically compare the two buffers because 5 mM BAPTA completely blocked fast exocytosis (24, 26).

The Slow Mode of Endocytosis Occurred at Resting Levels of Ca^{2+}. In the synaptic terminal of bipolar cells, an increase in stimulus duration leads to an increase in the proportion of membrane retrieved by slow endocytosis (12). An example of this effect is shown in Fig. 4*A Left*, which compares capacitance responses

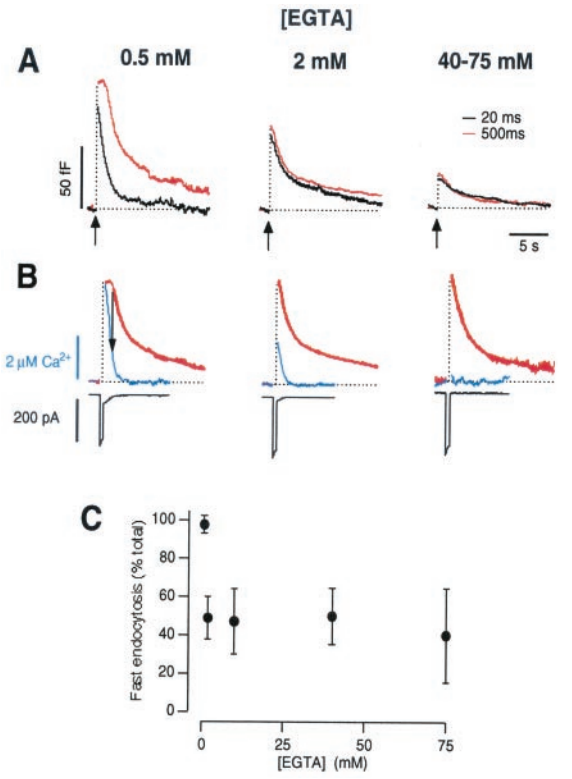

Fig. 4. Rises in global $[Ca^{2+}]$ altered the kinetics of endocytosis. (*A*) Capacitance responses in terminals loaded with 0.5, 2, and 40–75 mM EGTA. Compared are responses to stimuli of 20 ms (black traces) and 500 ms (red). Traces are averaged responses ($n = 6$, 7, and 12, respectively) and are unscaled. (*B*) The responses to the 500-ms stimuli from *A* scaled to the same maximum to allow comparison of their kinetics. The parameters of the fitted traces (bold) are shown in Table 2. The time course of endocytosis is also compared with the fall in $[Ca^{2+}]$, estimated from the Ca^{2+}-activated tail current using a conversion factor of 9 pA/μM (blue trace). The averaged Ca^{2+} currents that elicited these capacitance responses are shown below (black). In 0.5 mM EGTA, the fall in capacitance was not obvious until the free $[Ca^{2+}]$ fell below about ~1.5 μM (arrow). (*C*) The proportion of membrane retrieved by fast endocytosis as a function of the [EGTA] in the patch pipette. This analysis is confined to responses elicited by brief stimuli (including those shown by the black traces in *A*).

generated by 500 ms and 20 ms stimuli in the presence of 0.5 mM EGTA. Might the slow phase of endocytosis observed after the longer stimulus reflect an inhibitory action of Ca^{2+}? This possibility is suggested by reports that bulk rises in free $[Ca^{2+}]$ slow the rate constant of endocytosis in bipolar cells (19, 21). Fig. 4*B Left* compares the fall in membrane area after a long stimulus with the fall in free $[Ca^{2+}]$. To allow assessment of the free $[Ca^{2+}]$ from resting levels up to a few micromolar, we used the Ca^{2+}-activated tail current that gradually declined after closure of calcium channels (black trace in Fig. 4*B*; see *Materials and Methods* and ref. 24). Four observations indicate that the slow phase of endocytosis did not reflect an inhibitory action of Ca^{2+}. First, fast retrieval occurred when Ca^{2+} was highest. Second, the slow phase of endocytosis occurred after the $[Ca^{2+}]$ had returned to basal levels. Third, blocking rises in global $[Ca^{2+}]$ by the introduction of high concentrations of EGTA did not prevent slow endocytosis (Fig. 4*B Center* and *Right*). Finally, slow endocytosis was apparent after a brief stimulus was delivered in the presence of 40–75 mM EGTA.

An increase in stimulus duration altered the capacitance response in a second characteristic way: the fall in membrane surface area was delayed while the $[Ca^{2+}]$ was above about 1.5 μM (Fig. 4*B*; see also ref. 21). These two effects appeared to be

Table 2. Kinetics of endocytosis after a long stimulus

	Control	0.5 mM EGTA	2 mM EGTA	40–75 mM EGTA
A_{fast} (%)	65	40	46	50
τ_{fast} (s)	1.1	1.2	1.3	1.6
τ_{slow} (s)	10	24	34	38
n	15	6	10	7

The averaged time courses of the capacitance responses after a 500-ms depolarization were fit with the equation $A(t) = A_{fast} \cdot \exp(-t/\tau_{fast}) + A_{slow} \cdot \exp(-t/\tau_{slow})$. n is the number of terminals.

causally related, because increasing the concentration of EGTA to 2 mM or more reduced the rise in global $[Ca^{2+}]$ and also removed the delay before the fall in surface capacitance (Fig. 4*B Center* and *Right*). Several lines of evidence indicate that the delayed fall in capacitance after a prolonged stimulus is caused, at least in part, by the stimulation of "asynchronous" release by residual Ca^{2+}. First, capacitance measurements often showed a net increase in membrane surface area after a prolonged stimulus, as shown by the averaged responses obtained in 0.5 mM EGTA in Fig. 4*A* (see also ref. 12). Second, independent measurements of exocytosis using FM1–43 have demonstrated that exocytosis continues after a prolonged stimulus (12, 27). Consistent with these observations, a cytoplasmic $[Ca^{2+}]$ of the order of 1 μM can stimulate exocytosis at rates of more than 1,000 vesicles s^{-1} (19, 29).

Discussion

These results extend a previous characterization of fast and slow mechanisms of endocytosis at the synaptic terminal of bipolar

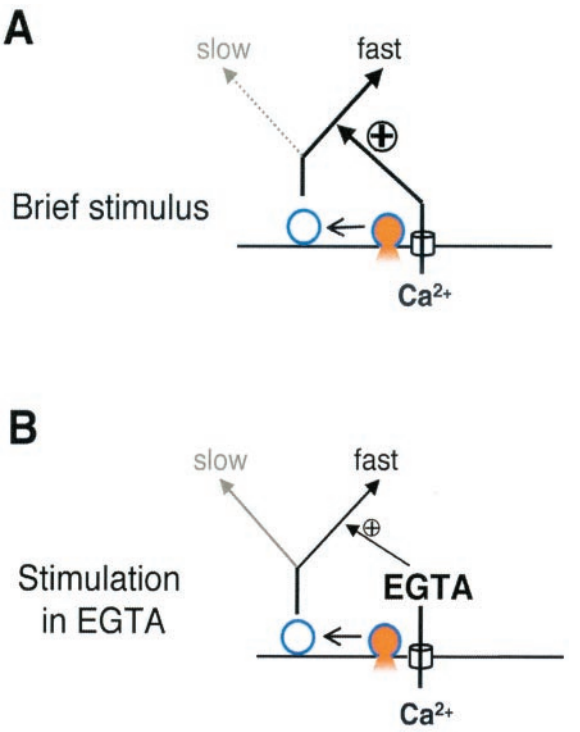

Fig. 5. A model to account for the kinetics of endocytosis and its modulation by calcium. (*A*) The localized Ca^{2+} signal generated by a brief stimulus normally causes all rapidly releasable vesicles (black) to be retrieved by the fast mode of endocytosis. (*B*) Excess EGTA suppresses the Ca^{2+} signal at the active zone, so only a fraction of vesicles are switched to the fast mode of endocytosis. Remaining membrane is retrieved by slow endocytosis. Note that EGTA *is* expected to buffer the Ca^{2+} signal at the active zone of bipolar cells (24).

cells (12) by demonstrating that Ca^{2+} influx is the signal selecting vesicles for the fast route of retrieval.

Regulation of Endocytosis by Ca^{2+}: A Model. Variations in the capacity of Ca^{2+} buffers, the amplitude of the Ca^{2+} current, or the duration of the stimulus all had the common effect of altering the proportion of membrane retrieved by fast endocytosis (Figs. 1, 2, and 4, Tables 1 and 2). The value of τ_{fast} was similar under all conditions tested, indicating that the speed of fast endocytosis was not modulated. These observations lead to the model shown in Fig. 5. There are two routes of endocytosis in the synaptic terminal of bipolar cells, fast ($\tau_{fast} \approx 1$ s) and slow ($\tau_{slow} \geq 10$ s). A Ca^{2+}-dependent process enables vesicles to be retrieved by fast endocytosis and the remainder are retrieved slowly. The local Ca^{2+} signal generated by a brief stimulus normally causes all vesicles that are released rapidly to be marked for fast endocytosis (Fig. 5*A*). Increasing the Ca^{2+}-buffering capacity of the terminal reduces the rise in free Ca^{2+}, so that only some released vesicles become marked for fast endocytosis (Fig. 5*B*).

It has been suggested that there is a single mechanism of endocytosis operates at the synapse of bipolar cells, which is inhibited by Ca^{2+} in a graded manner, with complete block at 1 μM Ca^{2+} (21). The present results demonstrate the existence of two kinetically distinct mechanisms of endocytosis and indicate that a local action of Ca^{2+} stimulates endocytosis by selecting vesicles for fast retrieval. The present results do not, however, rule out the possibility that the onset of fast endocytosis might be delayed while global [Ca^{2+}] is high (21). A proper evaluation of this idea is difficult, because exocytosis continues for some time after a prolonged stimulus and the capacitance technique only measures the net change in membrane surface area (12, 27). Nonetheless, when exocytosis (measured with FM1–43) is compared with the net change in membrane surface area (measured by using the capacitance technique) it does appear that the fast mode of endocytosis is inhibited during a long stimulus (12).

Why does a stimulus of increased duration lead to an increase in the proportion of membrane retrieved by slow endocytosis (12)? One possibility is that this difference reflects the different sites of vesicle fusion during prolonged stimulation. Total internal reflection fluorescence microscopy indicates that fast exocytosis in bipolar cells is localized to active zones, whereas long stimuli cause many vesicles to be released at sites remote from active zones (27). If fast endocytosis is also localized to the active zone, it would be expected to predominate after a brief stimulus, but not a long stimulus. Indeed, recent experiments have provided evidence for endocytic active zones close to exocytic active zones at motor nerve terminals (30, 31).

Fast and Slow Endocytosis at the Synapse. The idea that fast and slow forms of endocytosis might coexist at the synapse was first suggested by electron microscopic studies of the neuromuscular junction (4, 5). Electron microscopy also suggests that the rapid form of endocytosis is localized to the active zone (7, 30). The kinetics of fast and slow endocytosis were first measured directly by applying the capacitance technique to the giant synapse of bipolar cells (11, 12). A recent study using the capacitance technique has also observed fast and slow phases of endocytosis at the ribbon synapse of inner hair cells in the cochlea (13). The fast phase of retrieval was observed after the [Ca^{2+}] was raised above 15 μM by releasing caged Ca^{2+}, but it is unclear how endocytosis in hair cells might be modulated by normal influx of Ca^{2+} because a fast mode of retrieval has not been observed in response to a depolarizing stimulus (14).

Are fast and slow endocytosis at the bipolar cell synapse both clathrin-dependent processes or do they differ more fundamentally? The molecular mechanisms that underlie fast endocytosis at the synapse are controversial. Electron microscopy demonstrates that slow modes of endocytosis reflect the formation of clathrin-coated pits (4), but it has been suggested that fast endocytosis might reflect retrieval of vesicles that connect to the plasma membrane without fully collapsing (5, 7). Such a mechanism is often termed "kiss-and-run," and one form of this model proposes that the connection is an aqueous pore that opens to release the neurotransmitter but rapidly closes before the vesicle is retrieved (6, 17, 32). The molecular mechanisms of fast endocytosis remain to be elucidated. At the squid giant synapse, dynamin and synaptophysin interact in the presence of high concentrations of Ca^{2+}, which may underlie a rapid mechanism of endocytosis that is independent of clathrin (33). The results in this article provide a direct demonstration that Ca^{2+} influx couples fast exocytosis and endocytosis at the synapse.

1. Katz, B. & Miledi, R. (1967) *J. Physiol. (London)* **189,** 535–544.
2. Zucker, R. S. (1996) *Neuron* **17,** 1049–1055.
3. Koenig, J. & Ikeda, K. (1989) *J. Neurosci.* **9,** 3844–3860.
4. Heuser, J. E. & Reese, T. S. (1973) *J. Cell Biol.* **57,** 315–344.
5. Ceccarelli, B., Hurllbut, W. P. & Mauro, A. (1973) *J. Cell Biol.* **57,** 499–524.
6. Fesce, R., Grohovaz, F., Valtora, F. & Mendolesi, J. (1994) *Trends Cell Biol.* **4,** 1–4.
7. Koenig, J., Yamaoka, K. & Ikeda, K. (1998) *Proc. Natl. Acad. Sci. USA* **95,** 12677–12682.
8. Murthy, V. (1999) *Curr. Opin. Neurobiol.* **9,** 314–320.
9. Ryan, T. A. (1996) *Neuron* **17,** 1035–1037.
10. Angleson, J. K. & Betz, W. J. (1997) *Trends Neurosci.* **20,** 281–287.
11. von Gersdorff, H. & Matthews, G. (1994) *Nature (London)* **367,** 735–739.
12. Neves, G. & Lagnado, L. (1999) *J. Physiol. (London)* **515,** 181–202.
13. Beutner, D., Voets, T., Neher, E. & Moser, T. (2001) *Neuron* **29,** 681–690.
14. Moser, T. & Beutner, D. (2000) *Proc. Natl. Acad. Sci. USA* **97,** 883–888.
15. Ryan, T. A., Smith, S. J. & Reuter, H. (1996) *Proc. Natl. Acad. Sci. USA* **93,** 5567–5571.
16. Wu, L. G. & Betz, W. J. (1996) *Neuron* **17,** 769–779.
17. Klingauf, J., Kavalali, E. T. & Tsien, R. W. (1998) *Nature (London)* **394,** 581–585.
18. Sankaranarayanan, S. & Ryan, T. (2001) *Nat. Neurosci.* **4,** 129–136.
19. Rouze, N. C. & Schwartz, E. A. (1998) *J. Neurosci.* **18,** 8614–8624.
20. Cousin, M. & Robinson, P. (2000) *J. Neurosci.* **20,** 949–957.
21. von Gersdorff, H. & Matthews, G. (1994) *Nature (London)* **370,** 652–655.
22. Burrone, J. & Lagnado, L. (1997) *J. Physiol. (London)* **505,** 571–584.
23. Gomis, A., Burrone, J. & Lagnado, L. (1999) *J. Neurosci.* **19,** 6309–6317.
24. Burrone, J., Neves, G., Gomis, A., Cooke, A. & Lagnado, L. (2001) *Neuron*, in press.
25. Sakaba, T., Tachibana, M., Matsui, K. & Minami, N. (1997) *Neurosci. Res.* **27,** 357–370.
26. Mennerick, S. & Matthews, G. (1996) *Neuron* **17,** 1241–1249.
27. Zenisek, D., Steyer, J. & Almers, W. (2000) *Nature (London)* **406,** 849–854.
28. Neher, E. (1998) *Neuron* **20,** 389–399.
29. Lagnado, L., Gomis, A. & Job, C. (1996) *Neuron* **17,** 957–967.
30. Teng, H., Cole, J., Roberts, R. & Wilkinson, R. (1999) *J. Neurosci.* **19,** 4855–4866.
31. Roos, J. & Kelly, R. (1999) *Curr. Biol.* **9,** 1411–1414.
32. Stevens, C. F. & Williams, J. H. (2000) *Proc. Natl. Acad. Sci. USA* **97,** 12828–12833. (First Published October 24, 2000; 10.1073/pnas.230438697)
33. Daly, C., Sugimori, M., Moreira, J. E., Ziff, E. B. & Llinas, R. (2000) *Proc. Natl. Acad. Sci. USA* **97,** 6120–6125.